MAPPING MARS' SURFACE WINDS FROM THE GLOBAL DISTRIBUTION OF BARCHAN DUNES EMPLOYING ARTIFICIAL INTELLIGENCE L. Rubanenko[1], M.G.A Lapôtre[1], J. Schull[1], S. Pérez-López[1], L.K. Fenton[2], and R.C. Ewing[3]. [1]Stanford University, CA. [2]Carl Sagan Center, SETI, CA. [3]Texas A&M, TX. (liorr@stanford.edu)

Introduction: The surface of Mars is riddled with eolian landforms created by accumulating sand particles that are carried by the wind. When the sand supply is limited, these landforms tend to take the shape of isolated crescentic barchan dunes whose slipfaces are oriented in the dominant wind direction. As a result, analyzing the morphometrics of barchan dunes can help characterize the winds that formed them. Previous studies inferred the direction of prevailing surface winds from the orientation of dunes on Mars locally through manual analyses of spacecraft imagery [1, 2, 3]. However, building a global map remained challenging, as manual detection of individual dunes over the entire Martian surface is impractical. Automatic techniques based on traditional computer vision algorithms are largely ineffective at identifying the outlines of dunes from images, due to the difficulty to separate the feature of interest from the background - even with the aid of advanced statistics [4]. Although topography may assist the detection process, it is often not available at the required resolution. Here we employ a state of the art instance segmentation neural network - a type of artificial intelligence algorithm - to detect and analyze isolated barchan dunes on a global scale. The algorithm we use, Mask R-CNN (Regional Convolutional Neural Network) [5], accurately detects dunes and their outlines, which are automatically analyzed to extract the directions of the dominant wind and net sand-flux vectors. Our trained network currently supports the detection of isolated barchans and Transverse Aeolian Ridges (TARs), and can be generalized to detect other types of eolian bedforms.

Dune Detection Method: Traditional computer vision object detection algorithms apply a wide range of mathematical transformations to identify edges, corners, or well-defined geometric shapes within an image. In realistic conditions, these methods typically underperform a human interpreter, and are considered unreliable for many purposes. In recent decades, artificial neural networks have revolutionized object detection in images. This family of deep supervised machine learning techniques achieves abstraction comparable to that of humans by stacking layers of parameters given as inputs to non-linear activation functions. Each layer in the model extracts higher-level features from the previous layer: the first layers usually learn simple features such as edges or corners, and deeper layers can identify more abstract features such as faces, animals or letters and numbers. Here, we employ Matterport's implementation of Mask R-CNN [5, 6], an instance segmentation neural network, to detect, classify, and mask eolian landforms on Mars. As a proof of concept, our study focuses on the detection of barchan dunes, which are typically isolated and have a distinct shape, to extract surface wind directions on a global scale on Mars. In order to train the model, we extract images of dune fields obtained by the Mars Reconnaissance Orbiter Context Camera (MRO CTX) [7]. Images of dune fields were located using the global dune field catalog [8], standardized and cropped to a resolution of 832×832 pixels. Using Labelbox's online instance segmentation platform we labeled over 5000 instances of eolian features in 1008 images, subsequently employing image augmentation and weight decay to prevent overfitting [9].

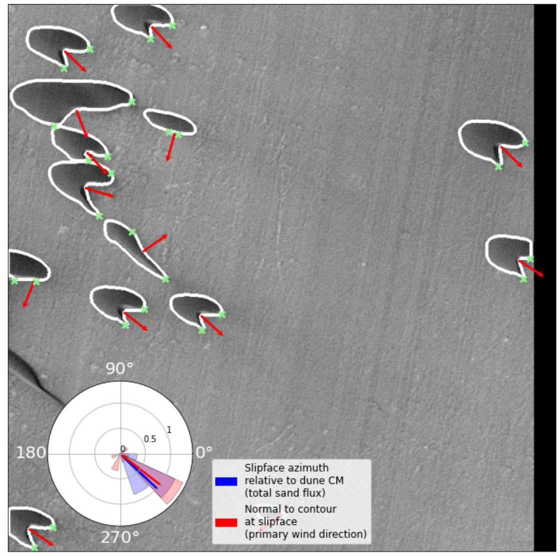

Figure 1: Dunes ($-28.89°$E, $-44.22°$N) and their contours produced by our detection algorithm. Red arrows indicate the vector normal to the slipface. The bars in the rose diagram show the distribution of the dominant wind direction (red) and net sand-flux (blue), and the dials indicate the mean of the distribution.

Deriving Wind Direction: When winds are unidirectional, the horns of barchan dunes tend to be symmetric, whereas bimodal wind regimes with divergence angle $> 90°$ tend to create asymmetric barchan dunes, with one horn elongating in the direction of the net sand-flux. Less commonly, horn asymmetry may also be caused by discontinuity in the surface slope, dunes collision, or influx asymmetry [10, 11]. In order to derive the dominant wind direction and the net sand-flux, we combine crestline-orientation and horn-geometry statistics within fields of barchan dunes. When both vectors (dominant wind and net sand flux) are aligned, a unimodal wind regime is inferred. First, we determine the vector normal to the slipface of individual dunes as a proxy for the dominant wind direction. To this end, we find the bisector of the head angle of a triangle that is formed by the dune slipface and the horns' apices (shown in Figure 1 as green X's). To detect the center of the slipface, we run a convexity defect algorithm which works by finding the maximum distance between the convex hull of the contour and the contour itself. To detect the horn apices, we calculate the second derivative of the dune contour, starting from the slipface. To determine the net sand-flux direction we use the azimuth of the slipface relative to the dune center of mass. This approach has not been used before to our knowledge, but appears to produce robust results. Groundtruthing of our methodology with data from terrestrial dune fields will be presented at the conference.

Results: We manually inspected 100 randomly selected images and found that our detection neural network correctly identified (true positive) $86 \pm 5\%$ of the isolated barchan dunes. The algorithm falsely identified a feature as a barchan dune (false positive) in only one single image. To illustrate our inferred wind directions, we present rose diagrams showing the polar distribution of the vector normal to the slipface of the dunes in the field, thought to roughly reflect the dominant wind direction (red bars in Figure 1), and the azimuth direction of the slipface center relative to the center of mass, which robustly aligns with the net sand-flux direction (blue bars in Figure 1). The dials in the rose diagrams show the averages of these distributions, weighted by the certainty that the detected object is a barchan dune (as outputted by the neural network) and that the detected location of the slipface is correctly identified and not some other convex defect. The latter is estimated by dividing the depth of the convexity defect by the size of the dune. To demonstrate the efficacy of our algorithm, we show two examples: a field of symmetric barchan dunes (Figure 2), in which the horns are roughly symmetric, and a field of asymmetric dunes, where the barchans elongate in the net sand-flux direction through a fingering instability (Figure 3). For symmetric barchans, the wind was inferred to be unidirectional as the dominant wind component and the net sand-flux are aligned to the northwest. In contrast, the asymmetric barchans indicate a net sand-flux towards the northeast and southerly dominant wind direction.

Conclusions: We employed a state of the art convolutional neural network to detect the outlines of individual barchan dunes on Mars and infer wind direction. Next, we will validate our wind-mapping methodology with groundtruthed data from terrestrial dune fields. Finally, we will expand our analysis to map surface winds globally on Mars. We expect our future dataset to serve as a constraint for atmospheric circulation models, and thus to help predict weather for upcoming in situ missions as well as shed new light onto the recent climate history of Mars.

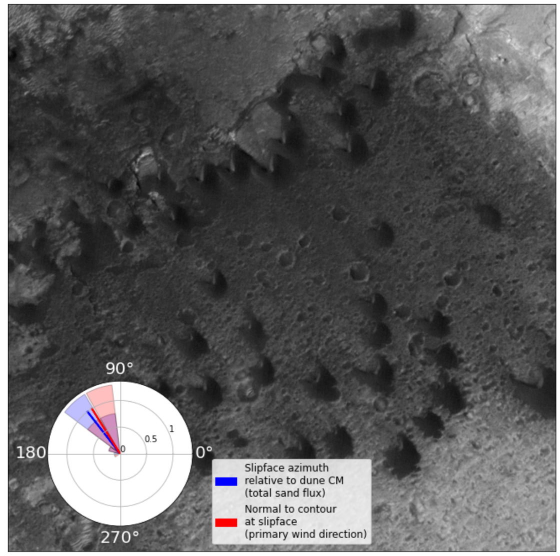

Figure 2: Example field of symmetric barchan dunes ($-53.67°$E, $6.79°$N), with inferred dominant wind and net sand-flux directions (here roughly aligned).

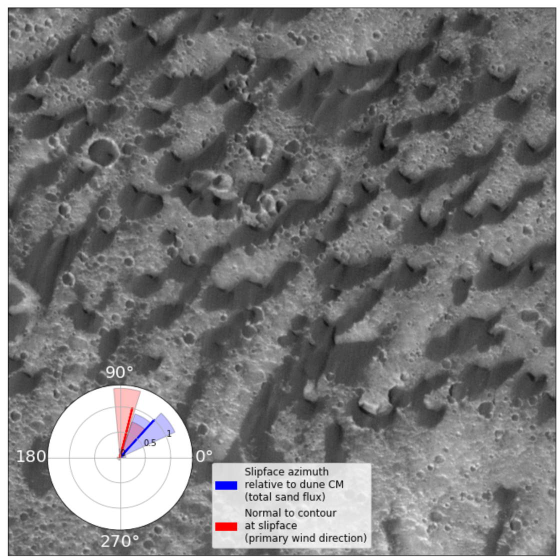

Figure 3: Example field of asymmetric barchan dunes ($-19.96°$E, $13.06°$N). Here, the dominant wind and net sand-flux are not aligned. Instead, the elongation of the horns indicates that the net sand-flux is to the north-east, whereas the dominant wind direction is southerly.

References: **[1]** Tsoar et al. *JGR* (1979). **[2]** Lee et al. *JGR* (1995). **[3]** Hayward et al. *Icarus* (2014). **[4]** Carrera et al. *Knowledge-Based Systems* (2019). **[5]** He et al. *IEEE CV*. 2017. **[6]** Abdulla. *Matterport* (2017). **[7]** Dickson et al. *LPSC*. 2018. **[8]** Fenton. *Icarus* (2020). **[9]** Shorten et al. *Journal of Big Data* (2019). **[10]** Parteli et al. *Aeolian Research* (2014). **[11]** Ping et al. *EES* (2016).